Supporting Information

Ultrasound triggered in situ photons emission for noninvasive optogenetics

Wenliang Wang,[a,1] Xiang Wu,[b,c,1] Kai Wing Kevin Tang,[a,1] Ilya Pyatnitskiy,[a] Rayna Taniguchi,[a] Peter Lin,[a] Richard Zhou,[a] Sam Lander C. Capocyan,[a] Guosong Hong, [b,c*] Huiliang Wang[a*]

a. Biomedical Engineering Cockrell School of Engineering, the University of Texas at Austin, Austin, TX, 78712, United States

b. Department of Materials Science and Engineering, Stanford University, Stanford, CA, 94305, United States

c. Wu Tsai Neurosciences Institute, Stanford University, Stanford, CA, 94305,United States

1. These authors contributed equally to this work.

*Corresponding author

Email: evanwang@utexas.edu, guosongh@stanford.edu

Keywords: Ultrasound, optogenetics, noninvasive, mechanoluminescence, ROS

Experimental Section/Methods

Materials： 1,2-dipalmitoyl-sn-glycero-3-phosphocholine (DPPC), cholesterol, 1,2-distearoyl-sn-glycero-3-phosphoethanolamine-N-[amino(polyethylene glycol)-2000] (DSPE-PEG_{2000}), IR-780 iodide (IR-780), L012 sodium salt (L012), 1,3-Diphenylisobenzofuran (DPBF), salicylic acid (SA) were ordered from Sigma-Aldrich. pGP-CMV-NES-jRGECO1a was a gift from Douglas Kim & GENIE Project (Addgene plasmid # 61563 ; http://n2t.net/addgene:61563 ; RRID:Addgene_61563). CheRiff_eGFP tet-on spiking HEK cells were purchased from ATCC. Rabbit anti-c-Fos antibody (1:1000 dilution, ab2222699), secondary antibody Goat anti-rabbit Alexa Fluor 594 (1:500 dilution, ab150080) and H&E staining kit were purchased from Abcam, and Donkey anti-rabbit Alexa Fluor 594 (1:500 dilution, A-21207) was purchased from Invitrogen. Hoechst 33342 (1:5000 dilution) was purchased from AAT Bioquest. Rabbit anti-Iba1 antibody (1:1000 dilution, 013-27691) was purchased from Wako Chemicals, and rabbit anti-Cleaved Caspase-3 (1:1000 dilution, 9664) was ordered from Cell signaling Technology.

Characterization: FEI TECNAI G2 F20 X-TWIN Transmission Electron Microscope (TEM) was used to evaluate the morphology of liposomes. The hydrodynamic diameter and surface potential of liposomes were evaluated through dynamic light scattering (DLS, Zetasizer Nano-ZS from Malvern Instruments). The UV-vis spectrum was measured via Eppendorf Biospectrometer. The mechanoluminescence spectrum was evaluated through Fluorolog3 Fluorimeter. The focused ultrasound (FUS) equipment was purchased from Image Guided Therapy. The fluorescence images and videos were recorded by Leica DMi8 fluorescence microscope.

Preparation of Liposomes. Thin film hydration strategy was used to prepare the liposomes.[1,2] In brief, 40 mg DPPC, 10 mg cholesterol, 4 mg DSPE-PEG_{2000} and 3 mg IR 780 were dissolved

in 10 mL mixed solution (chloroform : methanol, 5/1, v/v). The solvents were removed via vacuum distillation at 50 ℃ for 1 h to make thin film in 100 mL flask. Then, 5 mL $(NH_4)_2SO_4$ solution (200 mM) was added to dissolve the film. The mixture was sonicated at 60 ℃ water bath for 10 min to make sure the film was totally dispersed in solution, and extruded five times through 0.22 μm polycarbonate filter to homogenize the primary liposomes solution. Firstly, to prepare IR780 loaded liposomes (Lipo@IR780), the above solution was dialyzed against PBS (pH 7.4, 1 L) for 6 h to obtain Lipo@IR780, where the PBS was replaced each 2 h. In addition, to prepare IR780 and L012 coloaded liposomes (Lipo@IR780/L012), 5 mL Lipo@IR780 solution was incubated with L012 (1mg/mL) at 60 ℃ for 30 min. Then, the mixture was dialyzed against 1 L PBS (pH 8.5) for 4 h to remove uploaded L012, where the PBS was replaced each 2 h. 1 mL Lipo@IR780 and 1 mL Lipo@IR780/L012 was lyophilized to calculate the drug loading content of IR780/L012 through UV-Vis calibration curve (**Figure S1d** and **S1e**). 1 mg/mL liposome solution was used to prepare TEM samples and for the DLS tests, including the hydrodynamic size and zeta potential.

Stability tests of Liposomes. 10% FBS solution was used to mimic the body fluid. Lipo@IR780/L012 liposomes (1 mg/mL) were mixed with 10% FBS solution, after incubating at 37 ℃ for 4 h, the solution was tested via DLS to evaluate the stability. In addition, we also evaluate the stability of Lipo@IR780/L012 under the FUS stimulation according to the previous method.[3] 1 mg/mL Lipo@IR780/L012 solution was treated under the FUS irradiation (1.5 MHz, 1.5 MPa). 0.2 mL solution was extracted out at fixed time, and then centrifuged at 15000 rpm for 5 min. The supernatant was taken for UV-Vis tests to determine the leakage amount of IR780. Moreover, after FUS stimulation, the treated solution was taken to measure the size of nanoparticles via DLS.

Detection of the generation of $^1O_2$. 1 mL Lipo@IR780 (1 mg/mL) or Lipo@IR780/L012 (1 mg/mL) with 30 μL 1mg/mL DPBF (dissolved in methanol) were mixed. The UV-Vis characteristic absorption peak of DPBF at 420 nm was used to track the generation of $^1O_2$. The mixture was treated with or without FUS irradiation (1.5 MHz, 1.5 MPa), and extracted out 10 μL for UV-Vis spectrum tests. The absorbance change of DPBF at 420 nm was used to quantify the generation of $^1O_2$. Similarly, in order to quantify the generation of $^1O_2$ under the different FUS power density, we treated the mixture at different amplitudes (1.5 MHz, amplitude from 0 ~ 60%). The peak pressure was tested via hydrophone (Onda Corporation, HGL-0200).

Detection of the generation of •OH. 1 mL Lipo@IR780 (1 mg/mL) or Lipo@IR780/L012 (1 mg/mL) with 50 μL 1mg/mL SA (dissolved in methanol) were mixed. SA is one kind of typical •OH probe. The UV-Vis characteristic absorption peak of SA at 297 nm was used to track the generation of •OH. The mixture was treated with or without FUS irradiation (1.5 MHz, 1.5 MPa), and extracted out 10 μL for UV-Vis spectrum tests at fixed time. The absorbance change of SA at 297 nm was used to quantify the generation of •OH. Similarly, in order to quantify the generation of •OH under the different FUS power density, we treated the mixture at different amplitudes (1.5 MHz, amplitude from 0 ~ 60%).

Ultrasound peak pressure calibration. Measurement of the peak pressure provided by the transducer (Image Guided Therapy System, 25mm diameter Concave Annular Transducer at 1.5MHz with focal spot at 15-25mm) was performed by submerging in to a water tank along with hydrophone (Onda Corporation, HGL-0200) connected to a pre-amplifier (Onda Corporation, AG-2010) with a gain of 20dB was aligned uniaxially at the designated focal spot of 18-20mm using 3-axis mechanical system (Image Guided Therapy System). The water tank was lined with acoustic absorbing material (Precision Acoustics, Aptflex F28) to prevent acoustic reflection along the walls toward the hydrophone. Transducer was tested

experimentally via sonication of 100ms pulse at 1.5MHz with varying amplitudes of 5% - 60% (**Figure S3**). Measured voltage signal via connection of hydrophone and amplifier to oscilloscope (Siglent Technologies, SDS1202X-E) was converted to peak pressure by equation below.

$$Peak\ Pressure\ (Pa) = \frac{V_{measured}}{G(f)M_c(f)\frac{C_H}{C_H + C_C + C_A}}$$

$V_{measured}$: Voltage measured in oscilloscope via hydrophone and preamplifier

$G(f)$: Gain of preamplifier (Onda Corporation AG-2010, G = 10 at 1.5MHz)

$M_c(f)$: End of cable nominal sensitivity of hydrophone (Onda Corporation HGL-0200, M_c = 45nV/Pa at 1.5 MHz)

C_H: Input capacitance of hydrophone (Onda Corporation HGL-0200, C_H = 13pF at 1.5 MHz)

C_C: Capacitance of right-angle connector between hydrophone and pre-amplifier (C_C = 1.6 pF)

C_A: Input capacitance of pre-amplifier (Onda Corporation AGL-2010, C_A = 6.3 pF at 1.5 MHz)

Deep tissue penetration evaluation of FUS. Two mice were sacrificed, and the head was collected for in vivo ultrasound peak pressure tests. Measurements of the thickness were performed using the bregma as a reference point. In order to test the peak pressure at different depths in the brain, the mouse brain was dissected into different sections and then mounted between the FUS transducer (Image Guided Therapy System) and the hydrophone (Onda Corporation, HGL-0200) aligned at the bregma. Measurements were performed with increments of 0.5 mm from the bregma to the anterior and posterior points of the skull using a single FUS pulse of 100 ms on and 900 ms off at 1.5 MHz. Of note, the focal length of our transducer (from the transducer surface to the focal point) is around 15 mm. We adjust the

distance between transducer surface and water balloon surface to be 10 mm, to achieve different tissue penetration.

Mechanoluminescence spectrum of Lipo@IR780/L012. 30% hydrogen peroxide was used to mimic the reactive oxygen species (ROS), where 1 mL Lipo@IR780/L012 (10 mg/mL) was mixed with 30% hydrogen peroxide (0.1 mL), and the mechanoluminescence spectrum was measured via Fluorolog3 Fluorimeter. ChR2 and ChiReff absorption spectra were referred from previous work,[4,5] and extracted via GetDataGraphDigitizer software.

FUS triggered blue light emission from Lipo@IR780/L012 solution. 1mL Lipo@IR780/L012 solution (10 mg/mL) was added into a 2 mL vial. The vial was fixed with iron support and touched with the water balloon of the FUS transducer (1.5 MHz). To avoid air bubbles, ultrasound gel was used to fill the gaps between the vial and water balloon. First, FUS was applied with a repetition frequency of 1 Hz, pulse 100 ms FUS on 900 ms FUS off, and the amplitude was changed from 20% to 60% to evaluate the influence of FUS power on light emission. Then, we fixed the FUS amplitude to 60 %, and change the pulse, including 100 ms FUS on 1000 ms FUS off, 300 ms FUS on 1000 ms FUS off, 500 ms FUS on 1000 ms FUS off and 1000 ms FUS on 1000 ms FUS off. Finally, we also changed the FUS repetition frequency at 1 Hz (50 ms FUS on, 950 ms FUS off), 2 Hz (50 ms FUS on, 450 ms FUS off), 4Hz (50 ms FUS on, 200 ms FUS off) and 8 Hz (50 ms FUS on, 75 ms FUS off) at 60% amplitude. The blue light emission was recorded through a monochrome CMOS camera (CS165MU1/M - Zelux® 1.6 MP Monochrome CMOS Camera, Throlabs). All the parameters were fixed to record the video, and the data were analyzed by Image J software.

Deep tissue penetration evaluation of Lipo@IR780/L012 solution. Pork skin was used to mimic the normal tissue. Different depth pork skin (3 mm, 5 mm, 10 mm and 15 mm) was

firstly placed in the water balloon with ultrasound gel covered, respectively. The vial loaded 1 mL Lipo@IR780/L012 solution (10 mg/mL) was then placed in the pork skin filling with ultrasound gel. After totally removing the bubbles and gaps, FUS was used to irradiate the nanoparticle solution (1.5 MHz, pulse 100 ms FUS on 900 ms FUS off, 60% amplitude). The emission was recorded through a monochrome CMOS camera for further analysis.

Blue light emission half-time evaluation of Lipo@IR780/L012 solution. 2 mL vial with 1 mL Lipo@IR780/L012 solution (10 mg/mL) was placed in the water balloon. After totally removing the bubbles and gaps, FUS was used to irradiate the nanoparticle solution (1.5 MHz, pulse 1000 ms FUS on 1000 ms FUS off, 60% amplitude) until no light emission. The emission was recorded through a monochrome CMOS camera, and the data was analyzed by Image J software.

Hemolysis tests of Lipo@IR780/L012 nanoparticles. The experiments were conducted according to the previous method.[6] Briefly, 0.5 mL fresh blood was obtained from the mouse heart and added into 10 mL PBS. The mixture was centrifuged at 8000 rpm/min for 5 min and washed the pallets with fresh PBS three times to obtain the red blood cells (RBCs). After that, the RBCs were resuspended with 2 mL PBS. 1 mL Lipo@IR780/L012 nanoparticles solution with different concentrations was mixed with 20 μL RBCs solution, and irradiated with FUS (2.45 MPa, 100 ms on 900 ms off, 20 circulations) or without FUS, then incubated at 37 ℃ for 2 h. Of note, 20 μL RBCs solution was added into 1 mL DI water as positive control and 1 mL PBS as negative control. Then, the mixture was centrifuged at 12000 rpm for 5 min. The supernatant was collected to measure the absorption intensity at 541 nm (microplate reader, BioTek Synergy H1), where the liposomes with similar concentration were used as blank. The hemolysis percentage was calculated according to the following equation:

Hemolysis percentage (%) = Absorbance of samples / absorption of positive control x 100%

Cell viability tests of Lipo@IR780/L012 nanoparticles. Human embryonic kidney 293 (HEK293T) cells were seeded into 96 well plates coated with 10 μg/mL Poly-L-Ornithine solution. After the confluency was around 90%, complete medium containing Lipo@IR780/L012 nanoparticles at various concentrations were added into the plate. Moreover, we also evaluated the cell viability of FUS treated Lipo@IR780/L012 nanoparticles. The Lipo@IR780/L012 solution was treated via FUS (1.5 MHz, 60% amplitude) for 60s, after that, the Lipo@IR780/L012 was added to complete medium with different concentrations and added into the plates. After incubation for 24 h, 10 μL of Cell-Titer blue reagent (Promega Corporation) was added into each well. Cells were incubated for another 4 h for fluorescence absorption tests via microplate reader (BioTek Synergy H1, 560ex/590em nm). The cell viability was calculated according to the following equation:[7,8]

Cell viability (%) = fluorescence intensity of sample/fluorescence intensity of control x 100%

In vitro **sono-optogenetic.** CheRiff_eGFP tet-on spiking HEK cells with constitutive expressed blue light-actived channel rhodopsin actuator, voltage-gated sodium channel $Na_V1.5$, and inducibly (tet-on) express $K_{ir}2.1$ were purchased from ATCC. The cells were cultured in Dulbecco's Minimal Essential Medium (DMEM) with 10 % FBS and 2 mM L-glutamine, and seed into the 24 well plates coated with 10 μg/mL Poly-L-Ornithine solution. After the confluency was around 90%, the medium was replaced of 0.5 mL fresh DMEM, and 50 μL Reduced Serum Medium (opti-MEM™) containing 2 μL Lipofectamine 2000 and 1 μg pGP-CMV-NES-jRGECO1a plasmids was added into the cells. After incubation for 4 h, the medium was replaced with complete DMEM. The cells were incubated for another 2 days for effective gene transfection. Then, the vial filling 1 mL Lipo@IR780/L012 solution (10 mg/mL) was fixed over the cells, and the FUS (1.5 MHz, pulse 100 ms FUS on 900 ms FUS off, 60% amplitude) was used to treat the solution to generate blue light. The red fluorescence signals

were recorded via Leica DMi8 fluorescence microscope. The fluorescence signal was analyzed by Image J software.

***In vivo* near-infrared (NIR) fluorescence imaging and light intensity determination**.

To determine the distribution of Lipo@IR780/L012 nanoparticles after intravenous injection, C57BL/6J mice (20-26 g; 4 weeks old; Jackson laboratory) were used to for in vivo imaging via FOBI imaging system (CELLGENTEK Co., Ltd.). 0.2 mL Lipo@IR780/L012 nanoparticles (10 mg/mL) were injected into the mouse through intravenous injection, and the NIR imaging was conducted at 15, 30 and 60 minutes after the injection.

Besides, we also determined the *in vivo* light intensity according to the previous method.[9] Two optical fibers (CFML12L05, Thorlabs) were inserted into the motor cortex (anteroposterior (AP) ±1.0 mm, mediolateral (ML) +0.5 mm, dorsoventral (DV) −0.5 mm), and one was then connected to a blue LED (LEDD1B-T-Cube LED Driver, Thorlabs), and another one was connected to FLIR Blackfly S BFS-U3-51S5M-C Camera. The photons from LED light at different power densities were recorded through the camera, where the photons number was analyzed by ImageJ software to make a light density calibration curve. Next, in order to determine the light intensity from Lipo@IR780/L012 under the FUS stimulation, the mice were anesthetized with 2.5% isoflurane, and fixed in a stereotaxic frame, and placed in a 37 ℃ heating pad to maintain body temperature. The eyes were protected via coating vet ointment. 0.2 mL Lipo@IR780/L012 (10 mg/mL in PBS) was injected through the tail vein. After 15 min, ultrasound transducer (1.5 MHz, Image Guided Therapy, France) was placed on the mice head with ultrasound gel filling the gaps. FUS was conducted with repetition frequency of 1 Hz (100 ms FUS on, 900 ms FUS off) and amplitude 60%, the photons from the nanoparticles were collected via the camera, and the light power was calculated according to a pre-tested light density calibration curve after correction.

***In vivo* sono-optogenetic stimulation with Lipo@IR780/L012 nanoparticles**.

Thy1-ChR2-YFP transgenic mice and C57BL/6J mice (20-26 g; 4 weeks old; Jackson laboratory) were used in our study. All procedures designed according to the National Institute of Health Guide for the Care and Use of Laboratory Animals, approved by the Institutional Animal Care and Use Committee at the University of Texas at Austin, and were supported via the Animal Resources Center at University of Texas at Austin. The mice were anesthetized with 2.5% isoflurane, and cut the hair on the head of mice by hair clipper. After that, the mice were fixed in a stereotaxic frame, and placed in a 37 ℃ heating pad to maintain body temperature. The eyes of the mouse were protected via coating vet ointment. 0.2 mL Lipo@IR780/L012 (10 mg/mL in PBS) was administered through the tail vein.

After injection of Lipo@IR780/L012 nanoparticles, ultrasound gel was placed on the mouse head at first, and then the FUS transducer (1.5 MHz, Image Guided Therapy, France) with 5 mm water balloon was placed on the top of the gel. To achieve effective FUS stimulation, please make sure there are no gaps and bubbles between the transducer and brain, and the gel was totally filled. The stereotaxic coordinates of the motor cortex were anteroposterior (AP) ±1.0 mm, mediolateral (ML) +0.5 mm, dorsoventral (DV) −0.5 mm.[10] Then, the isoflurane concentration was adjusted to 0.5%. To guarantee the mouse was in light anesthesia status before conducting the FUS stimulation, we pinched the toes of the mouse to check the response. The FUS stimulation could be started until we observe the body movement when pinching the toes of the mouse. FUS was conducted with repetition frequency of 1 Hz (100 ms FUS on, 900 ms FUS off) and amplitude 60%, while the motions of the limbs were recorded through video camera during the FUS stimulation.

Histology.

(a) c-Fos staining. Thy1-ChR2-YFP transgenic mice were conducted following *in vivo* sono-optogenetic stimulation procedures at first. After 90 min, the mice were anesthetized and

transcardially perfused with 1 x PBS and 4% paraformaldehyde. The mice brains were extracted and stored at 4% paraformaldehyde overnight for section. The brain slices were washed 3 times with 0.3% Triton-X PBS solution, and blocked with 1 mL 10% normal goat serum/0.3% Triton-X in PBS for 30 min at room temperature. Then, the blocking buffer was replaced by rabbit anti-c-Fos antibody (1:1000 dilution)/0.3% Triton-X in PBS. After incubated overnight at 4 ℃, the slices were washed with 0.3% Triton-X PBS solution three times, and fresh 0.3% Triton-X PBS solution with secondary antibody Goat anti-rabbit Alexa Fluor 594 (1:500 dilution) and Hoechst 33342 (1:5000 dilution) was added and incubated for 1 h at room temperature. Finally, slices were washed three times with PBS before they were mounted on slides with coverslips. Fluorescence images were acquired on Zeiss 710 laser scanning microscope.

(b) Iba1 and Caspase-3 staining. Thy1-ChR2-YFP transgenic mice were treated with *in vivo* sono-optogenetic stimulation procedures at first. After 7 days, the mice were anesthetized and transcardially perfused with 1 x PBS and 4% paraformaldehyde. Similar with the c-fos staining procedures except the antibodies. The brain slices were washed 3 times with 0.3% Triton-X PBS solution, and blocked with 1 mL 10% normal donkey serum/0.3% Triton-X in PBS for 30 min at room temperature. Then, the blocking buffer was replaced by rabbit anti-Iba1 antibody (1:1000 dilution)/0.3% Triton-X in PBS or rabbit anti-Cleaved Caspase-3 antibody (1:1000 dilution)/0.3% Triton-X in PBS. After incubated overnight at 4 ℃, the slices were washed with 0.3% Triton-X PBS solution three times, and fresh 0.3% Triton-X PBS solution with secondary antibody Donkey anti-rabbit Alexa Fluor 594 (1:500 dilution) and Hoechst 33342 (1:5000 dilution) was added and incubated for 1 h at room temperature. Finally, slices were washed three times with PBS before they were mounted on slides with coverslips. Fluorescence images were acquired on a Leica DMi8 fluorescence microscope.

(c) H&E staining. Thy1-ChR2-YFP transgenic mice were treated with *in vivo* sono-optogenetic stimulation procedures at first. After 7 days, the mice were anesthetized and transcardially perfused with 1 x PBS and 4% paraformaldehyde. The mice organs (heart, liver, spleen, lung, kidney and brain) were extracted and immersed in 4% paraformaldehyde overnight for section. 10 μm slices were acquired for H&E staining. The images were captured with a Nikon Eclipse Ni Compound Light Microscope. Cell nucleus density is an important feature for determining tissue pathology and tissue damage. [11,12] No changes in cell nucleus density was observed in different organs after nanoparticles/ultrasound stimulation.

Animal behavior tests data processing. Recorded video of the mices' response to ultrasound stimulations were synchronized for quantification of joint angle to determine response in sono-optogenetic stimulation across groups exposed to none, either, or both Lipo@IR780/L012 nanoparticles and ultrasound pulses. Kinematic data were obtained by using DeepLabCut (a markerless pose estimation algorithm based on transfer learning with neural networks for 2D and 3D videos). Images were segmented, down-sampled and extracted into batches of 20 images per video through the use of k-means algorithm as recommended for behavioral study for postures in kinematic data of extremities as opposed to uniform temporal sampling, which is more suitable for global movement of mice within an environment.[13] Position of the hip, knee, and joints of the mice were determined by initially labeling 400 images manually for both left and right legs (**Figure S11**). 380 of the labeled images (95%) was used for training the neural network model using the ResNet50 framework (commonly used pre-trained network for object recognition) and 20 of the labeled images (5%) were used for verification and evaluation at an iteration of 500,000 epochs. The predicted pose is evaluated with the validation set to determine the maximum error in prediction of the (x,y) coordinates in terms of pixels. Trained model error indicates an average 7.38 pixel and test error evaluated between predicted and

labeled pose yielded an error of 9.99 pixel, which yields an error of ±0.603 degrees. Extraction of orientation between marked segments (i.e. hip-to-knee / knee-to-foot) were obtained through calculating the relative segments between the two coordinate points in relation to the horizontal axis of the image. The orientation of segments yielding joint angle was differentiated with respect to time to determine the change in joint angles for quantifying the efficacy of Lipo@IR780/L012 subjected to FUS in mice. This is done by segmenting the data points during which FUS occurs and taking the difference between the maximum (positive) and minimum (negative) peaks and averaged across the groups.

Figures

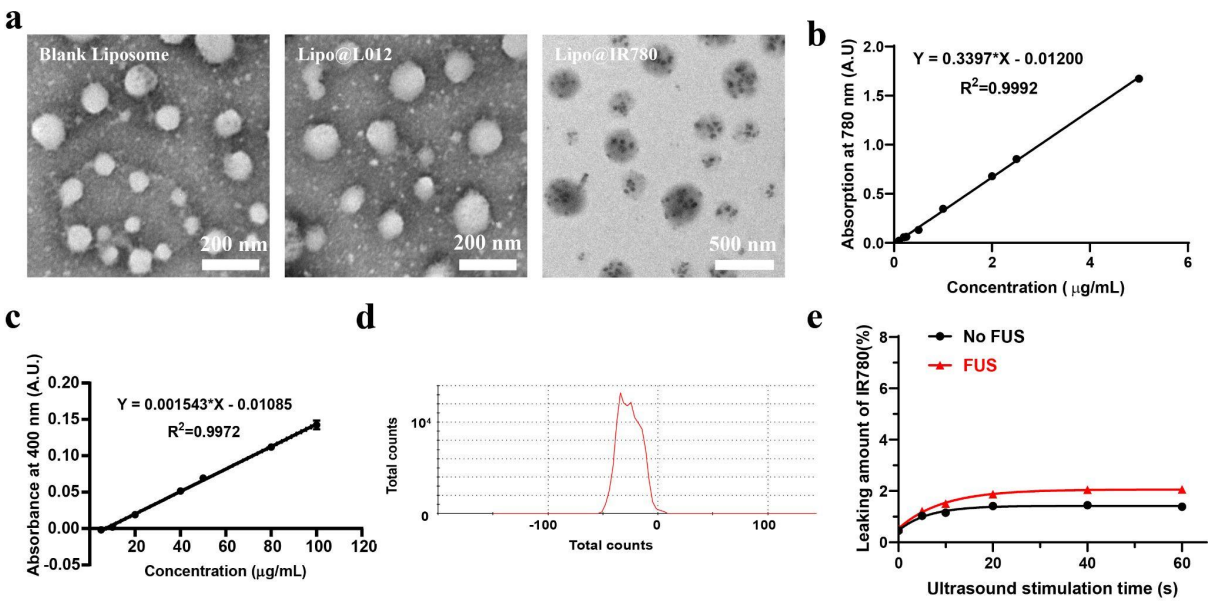

Figure S1. Characterizations of various liposomes. (a) TEM image of blank liposome; (b) the concentration calibration curve of IR 780 in methanol (n=3 per group); (c) the concentration calibration curve of L012 in water (n=3 per group); (d) the zeta potential of Lipo@IR780/L012 nanoparticles determined via DLS. All plots show mean ± SEM unless otherwise mentioned. (e) The leaking amount of IR780 from Lipo@IR780/L012 with or without FUS stimulation.

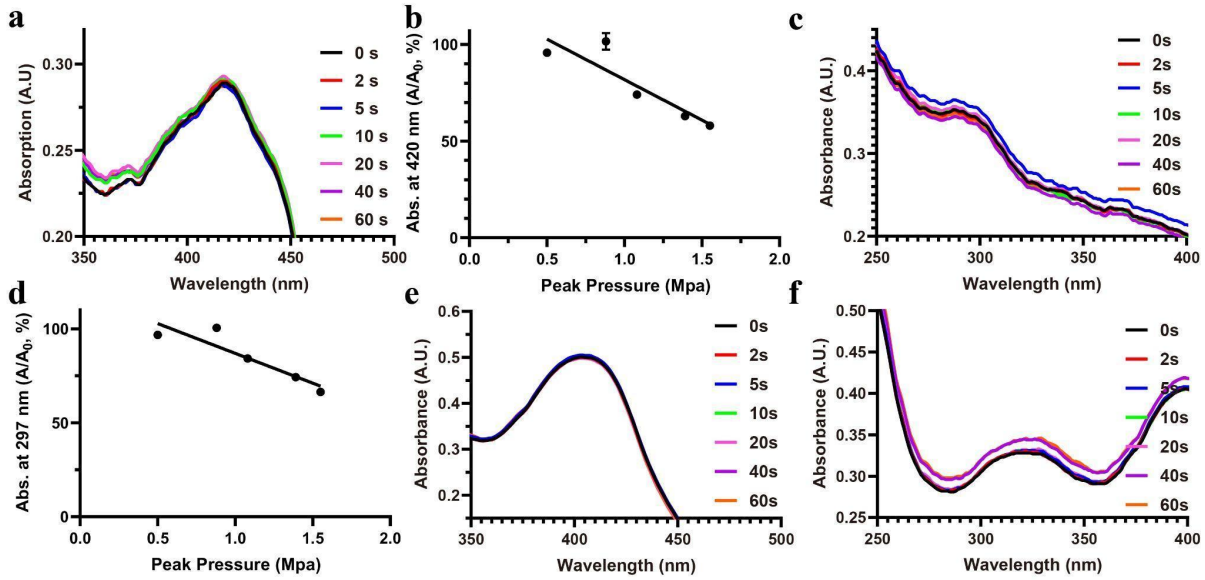

Figure S2. The ROS detection under the FUS irradiation. (a) time dependent UV-Vis degradation spectrum of DPBF indicating there was no $^1O_2$ generation via Lipo@IR780 nanoparticles without FUS irradiation; (b) quantification analysis of DPBF decomposition in presence of Lipo@IR780 under the different FUS peak pressure (n=3 per group); (c) time dependent UV-Vis degradation spectrum of SA indicating ·OH was not generated via Lipo@IR780 in absence of FUS (1.5 MHz, peak pressure 1.5 MPa); (d) the quantification analysis of SA decomposition in presence of Lipo@IR780 under the different FUS peak pressure (n=3 per group); (e) time dependent UV-Vis degradation spectrum of SA indicating there were no ·OH residues when Lipo@IR780/L012 nanoparticles were treated via FUS (1.5 MHz, peak pressure 1.5 MPa);(f) quantification analysis of SA decomposition in presence of Lipo@IR780/L012 with/without FUS irradiation. All plots show mean ± SEM unless otherwise mentioned.

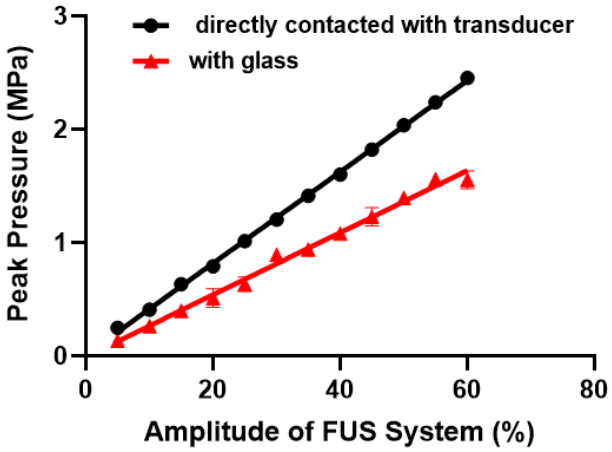

Figure S3. The calibration curve of peak pressure, where hydrophone is either directly contacted to transducer (black) or a piece of glass placed between hydrophone and the transducer (red) (n=3 per group). All plots show mean ± SEM unless otherwise mentioned.

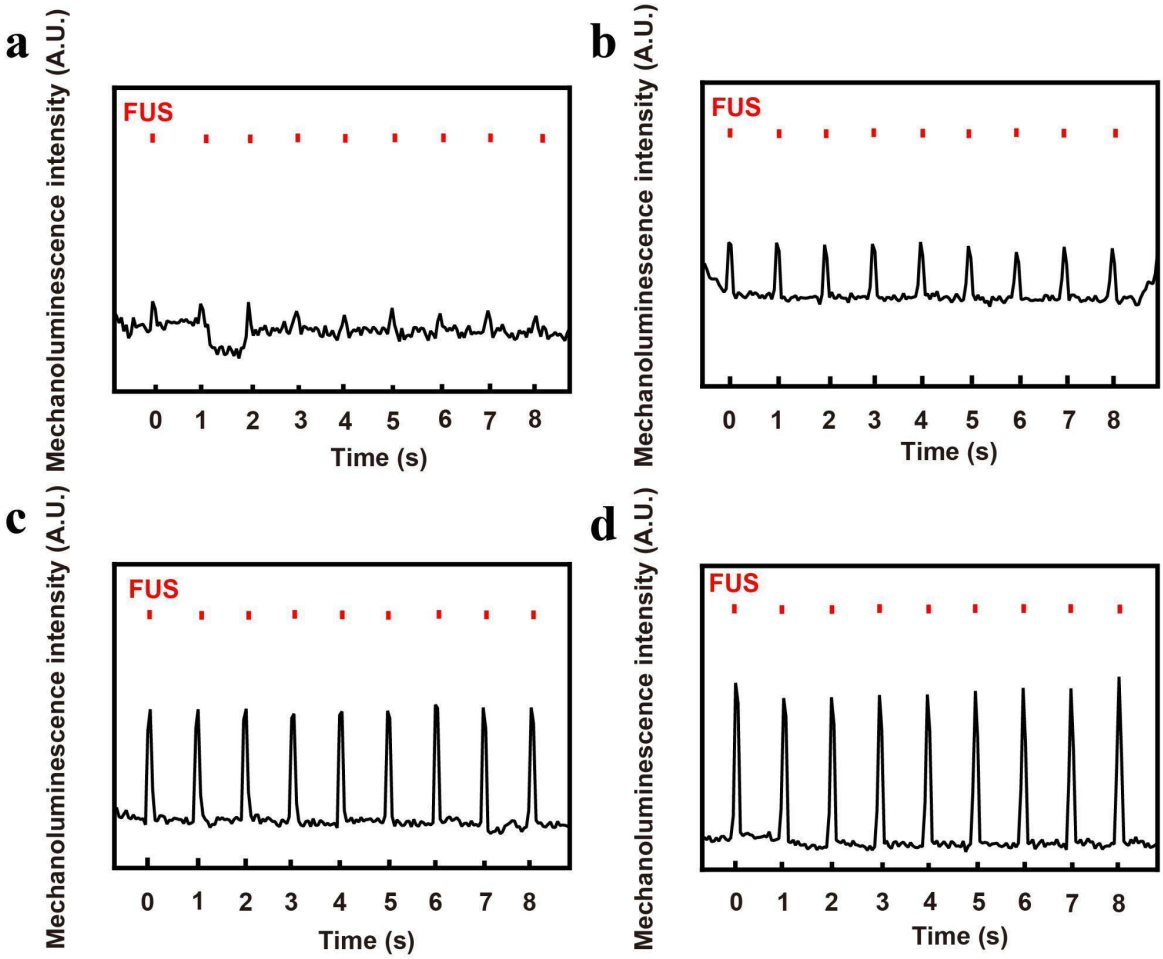

Figure S4. 470 nm blue light emission from Lipo@IR780/L012 nanoparticles under the FUS irradiation with different peak pressure (1.5 MHz, pulse 100 ms on, 900 ms off, 1 Hz). (a) 0.51 MPa; (b) 0.88 MPa; (c) 1.10 MPa; (d) 1.40 MPa.

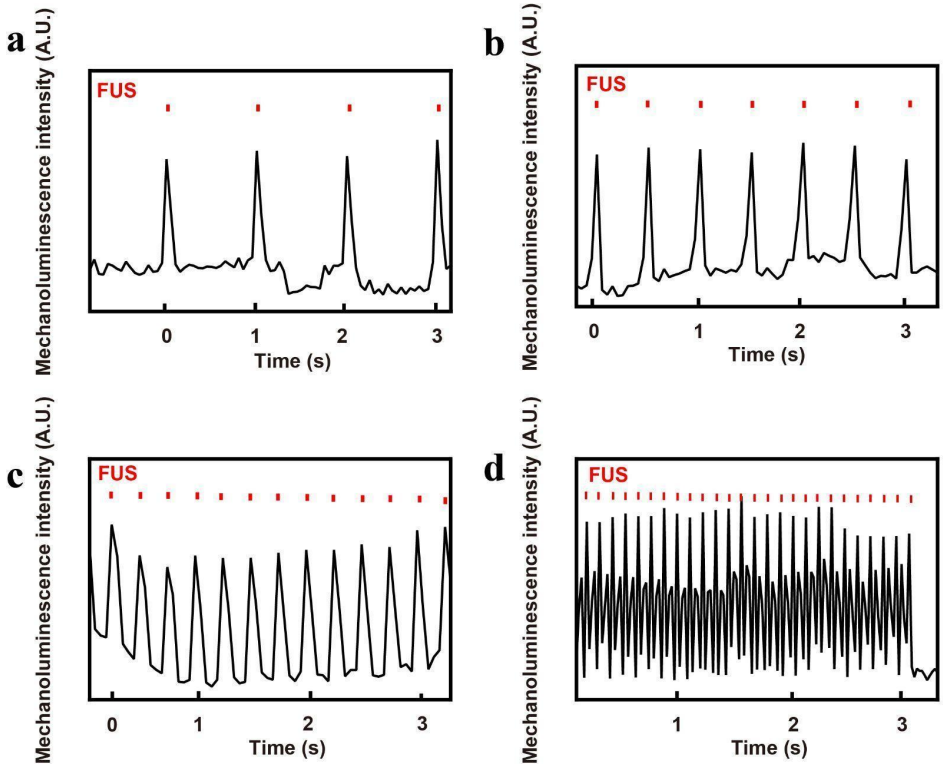

Figure S5. 470 nm blue light emission from Lipo@IR780/L012 nanoparticles under different frequency FUS pulse irradiation (1.5 MHz, 1.5 MPa). (a) 1 Hz (pulse 100 ms on, 900 ms off); (b) 2 Hz (pulse 100 ms on, 400 ms off);(c) 4 Hz (pulse 100 ms on, 150 ms off); (d) 8 Hz (pulse 50 ms on, 75 ms off).

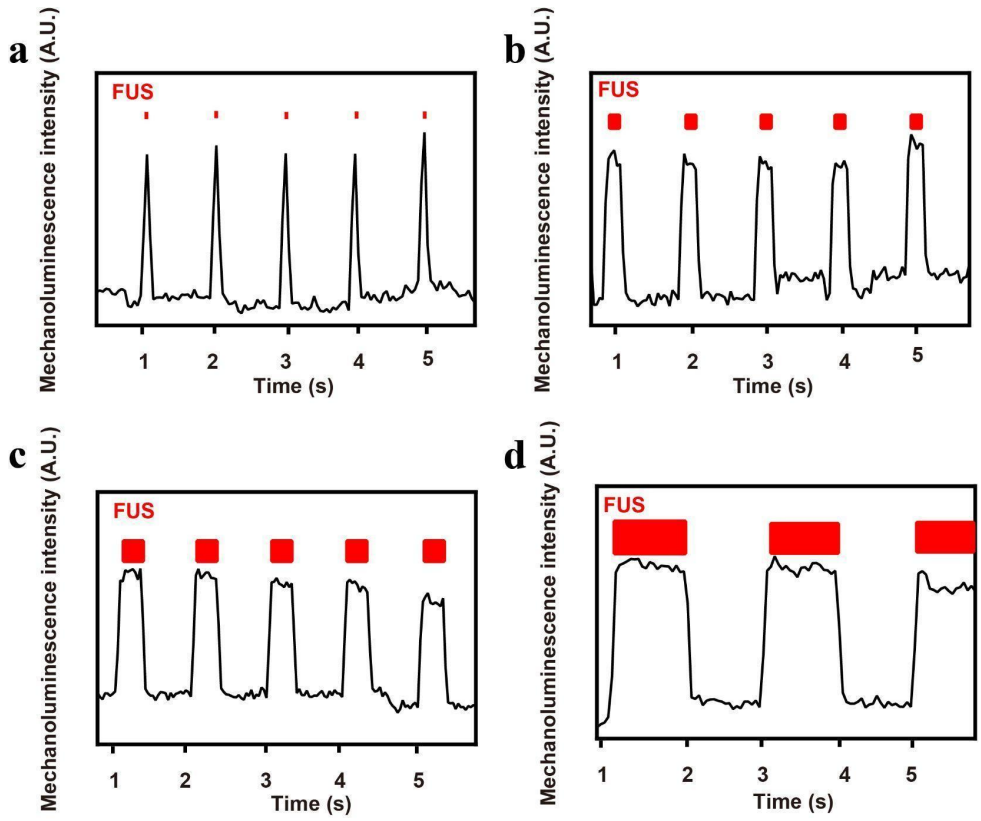

Figure S6. 470 nm blue light emission from Lipo@IR780/L012 nanoparticles under different pulse FUS irradiation (1.5 MHz, 1.5 MPa). (a) 100 ms (pulse 100 ms on, 1000 ms off); (b) 300 ms (pulse 300 ms on, 1000 ms off);(c) 500 ms (pulse 500 ms on, 1000 ms off); (d) 1000 ms (pulse 1000 ms on, 1000 ms off).

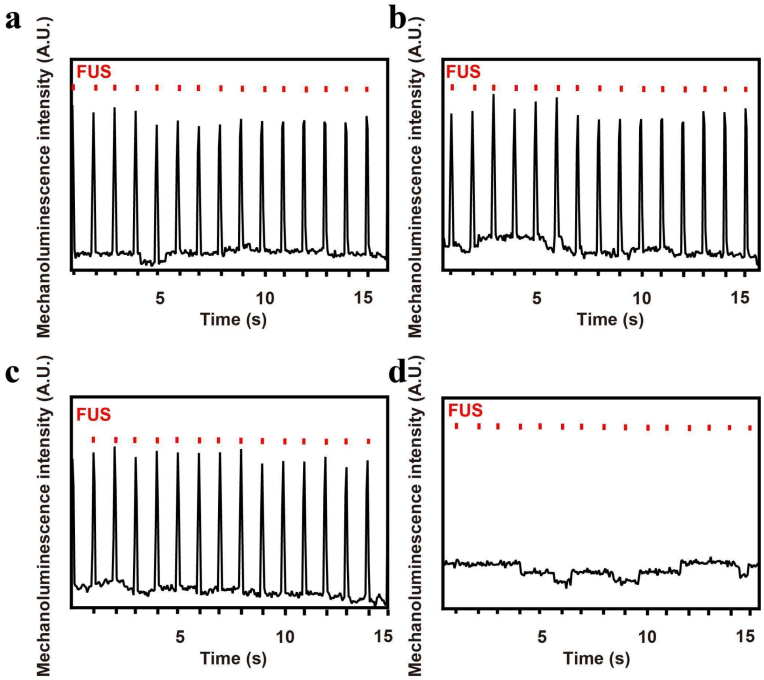

Figure S7. 470 nm blue light emission from Lipo@IR780/L012 nanoparticles in different depth pork skin under different pulse FUS irradiation (1.5 MHz, 1.5 MPa, pulse 100 ms on, 900 ms off). (a) there was no pork skin; (b) the pork skin depth was 3 mm; (c) the pork skin depth was 5 mm; (d) the pork skin depth was 15 mm.

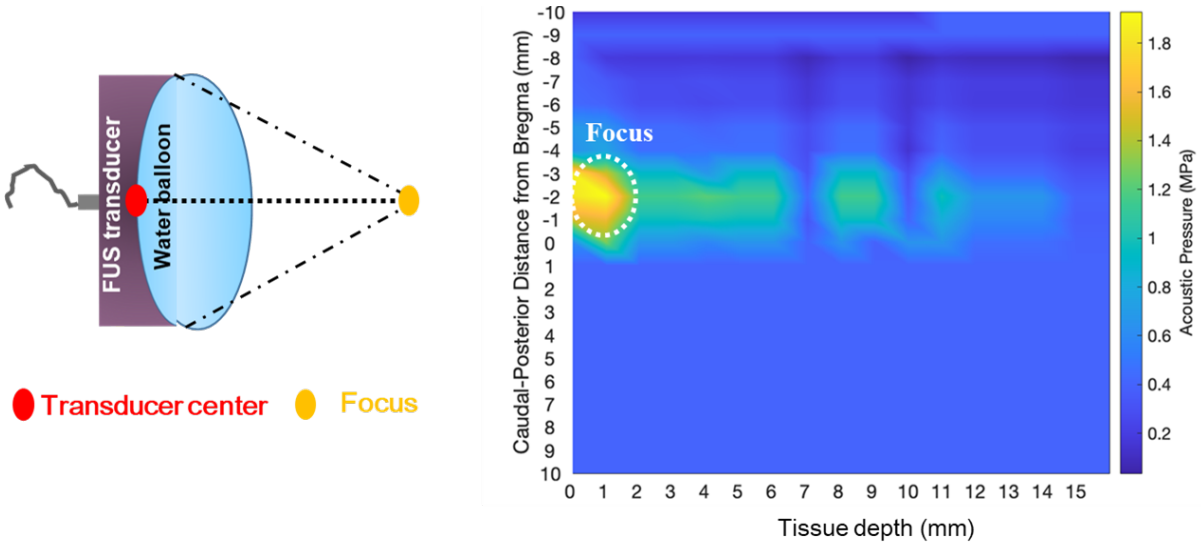

Figure S8. (a) The scheme of FUS focus; (b) The peak pressure at mouse brain tissue. We set the ultrasound focus to overlap with the motor cortex region, and then measured the ultrasound peak pressure at different depths in the brain through the mouse head skin, where 1.93 Mpa

peak pressure was achieved around the motor cortex when we use 2.45 MPa primary peak pressure. The mouse head was dissected into different sections and then mounted between the FUS transducer and the hydrophone. Measurements were performed with increments of 0.5 mm from the bregma to the anterior and posterior points of the skull using a single FUS pulse (100 ms on and 900 ms off, amplitude 60%).

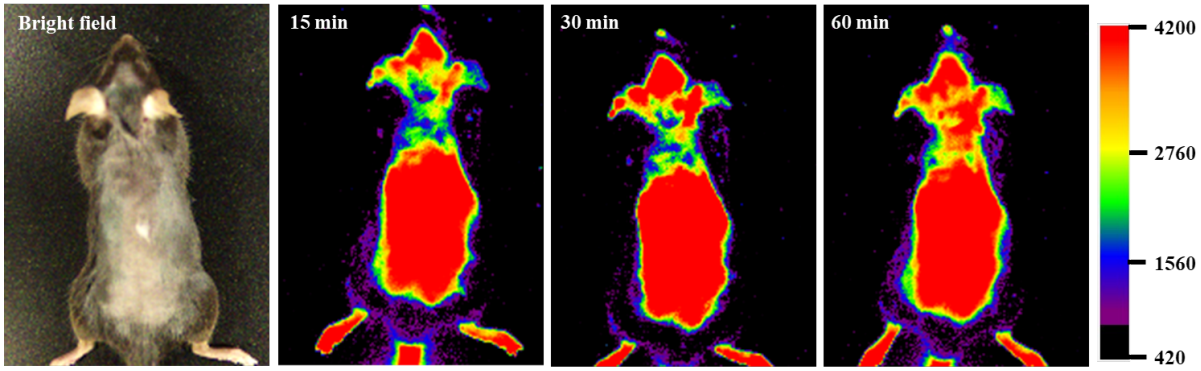

Figure S9. The *in vivo* NIR fluorescence imaging of mouse at 15, 30 and 60 minutes after intravenous injection of Lipo@IR780/L012.

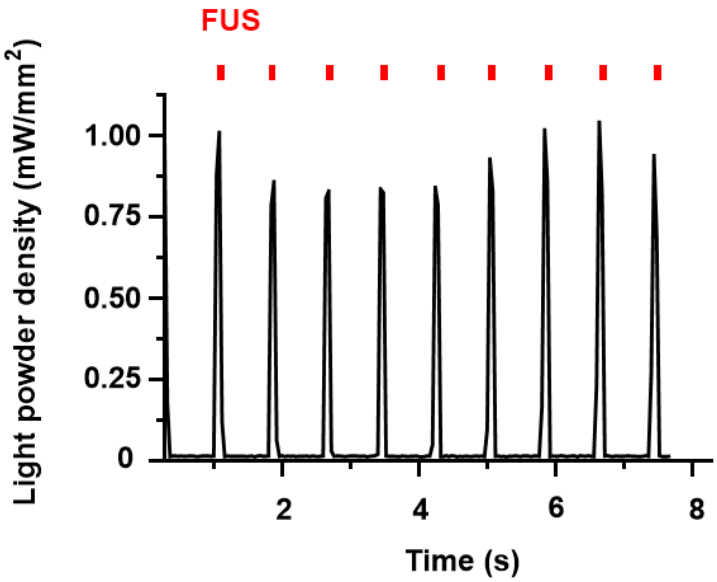

Figure S10. The blue light emission in the motor cortex from Lipo@IR780/L012 nanoparticles under the FUS irradiation.

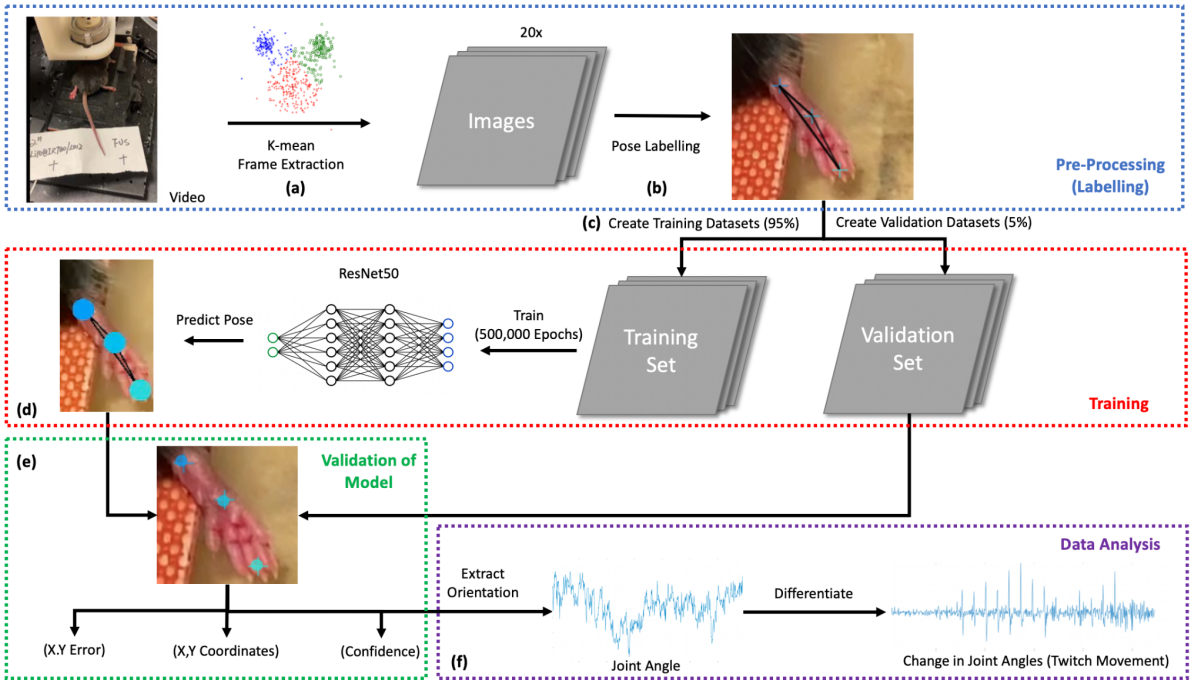

Figure S11. DeepLabCut framework in extracting kinematics data. (a) Images were segmented, down-sampled and extracted into batches of 20 images per video through the use of k-means algorithm; (b) Position of the hip, knee, and joints of the mice were determined by initially labeling 400 images manually for both lower extremities of the mice; (c) 380 of the labeled images (95%) was used for training the neural network model and 20 of the labeled images (5%) were used for verification and evaluation; (d) Training of the neural network model using ResNet50 was implemented for 500,000 epochs to ensure convergence of results. (e) The predicted pose was evaluated with the validation set to determine the maximum error in prediction of the (x,y) coordinates in terms of pixels; (f) Extracted (x,y) coordinates of the pose enables calculation of the segment orientation (joint angle) of interest yielding general movement. Differentiation of segment orientation with respect to time was followed to determine twitch movement as a result of ultrasound stimulation.

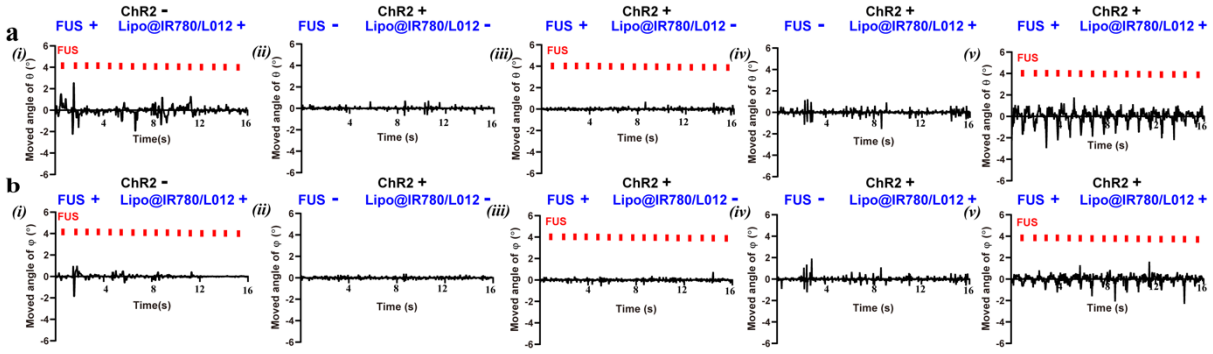

Figure S12. Time-resolved left limb's hip-knee response. (a) and knee-feet response (b) to FUS in first mouse group, (i) FUS (1.5 MHz, puls 100 ms on, 900 ms off, 1 Hz, 1.5 MPa), Lipo@IR780/L012, FUS (1.5 MHz, puls 100 ms on, 900 ms off, 1 Hz, 1.5 MPa), Lipo@IR780/L012 (ii) Thy1-ChR2-YFP transgenic mice, no FUS, no Lipo@IR780/L012 nanoparticles; (iii) Thy1-ChR2-YFP transgenic mice, FUS (1.5 MHz, puls 100 ms on, 900 ms off, 1 Hz, 1.5 MPa), no Lipo@IR780/L012 nanoparticles; (iv) Thy1-ChR2-YFP transgenic mice, no FUS, Lipo@IR780/L012 nanoparticles; (v) Thy1-ChR2-YFP transgenic mice, FUS (1.5 MHz, puls 100 ms on, 900 ms off, 1 Hz, 1.5 MPa), Lipo@IR780/L012.

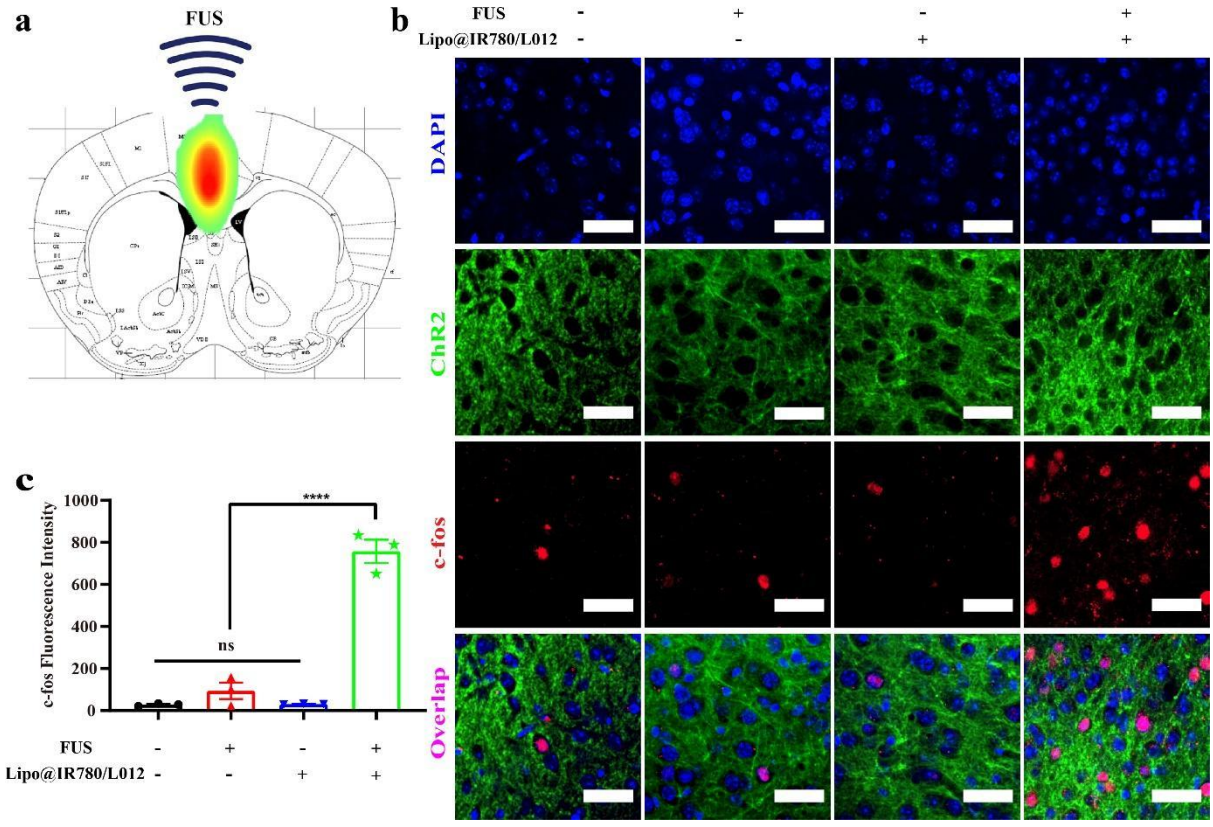

Figure S13. Immunohistology of motor cortex region after stimulation. (a) Schematic of *in vivo* sono-optogenetic at motor cortex; (b) fluorescence images of motor cortex region under different irradiation conditions. Remarkable c-fos (red fluorescence) was observed under the FUS irradiation with Lipo@IR780/L012 nanoparticle injection, Scale bar: 40 μm. (c) Statistical analysis for the fluorescence intensity of c-fos at different conditions (n=3 per group, two-way ANOVA). All plots show mean ± SEM unless otherwise mentioned. *P <0.05, **P<0.01, ***P<0.001, ****P<0.0001; ns, not significant.

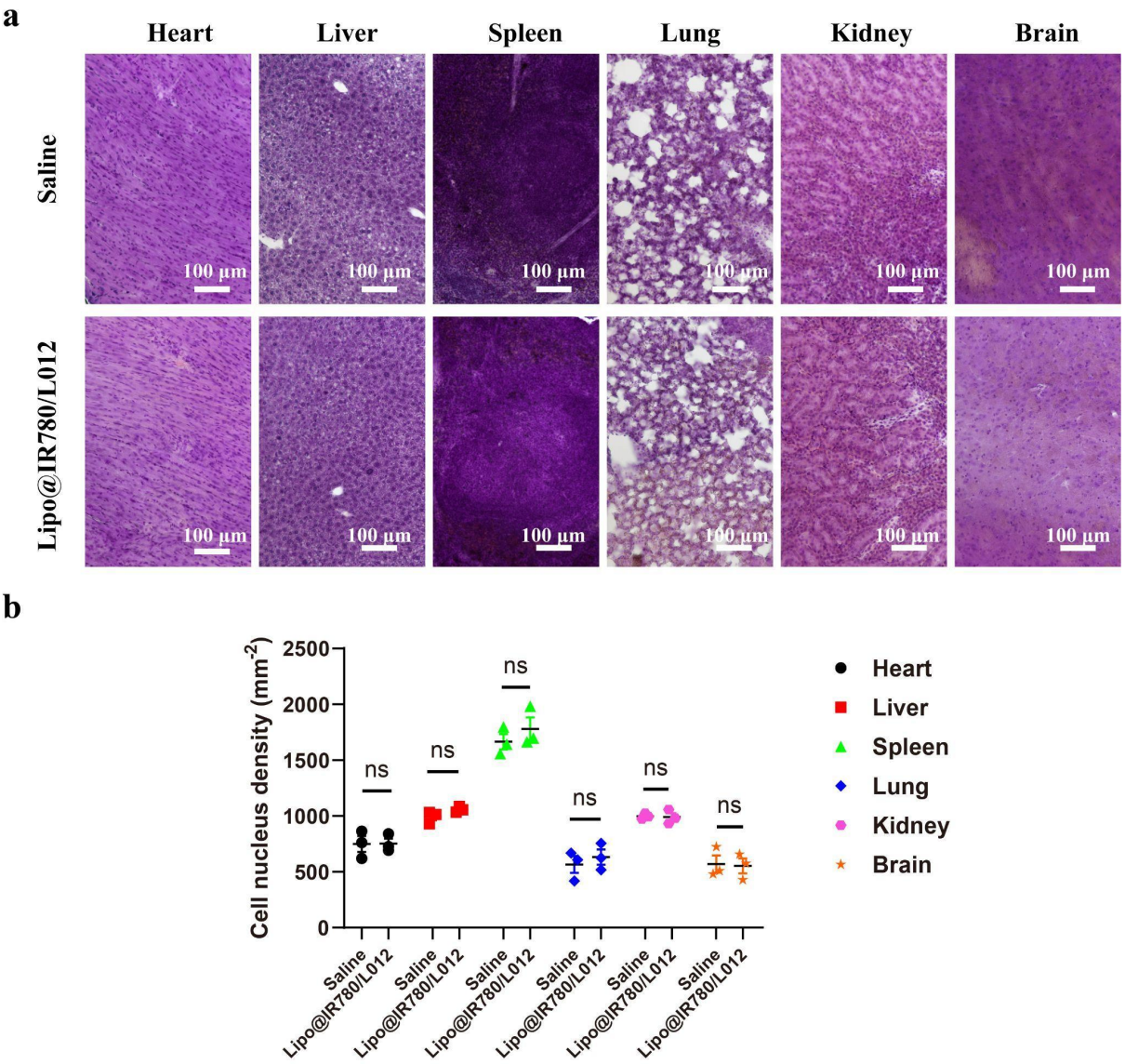

Figure S14. (a) H&E staining of organs treated at different conditions after 7 days (Saline and Lipo@IR780/L012 with FUS stimulation), Scale bar: 100 μm; (b) Quantification of cell nuclei from the H&E staining images. (n=3 per group, two-way ANOVA). After injection of

Lipo@IR780/L012 nanoparticles, FUS was conducted with repetition frequency of 1 Hz (100 ms FUS on, 900 ms FUS off) and amplitude 60%. Animals were sacrificed 7 days after stimulation. All plots show mean ± SEM unless otherwise mentioned. *P <0.05, **P<0.01, ***P<0.001, ****P<0.0001; ns, not significant.

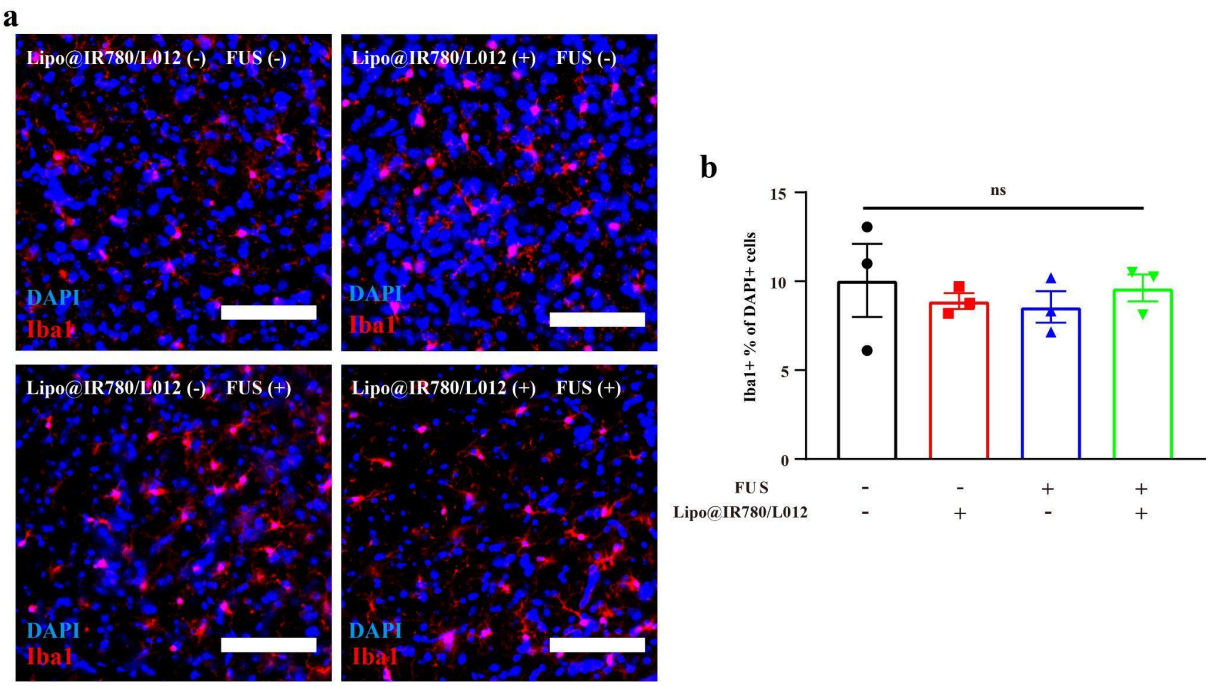

Figure S15. The biosafety assessment of our system in the motor cortex by immunostaining of Iba1 (marker of microglia activation). (a) The immunostaining images in motor cortex area under the different stimulations; Scale bar: 100 μm. (b) Percentages of Iba1 positive cells within the cell population indicated by DAPI (n=3 per group, two-way ANOVA), indicating there was no obvious glial activation induced under the treatment of this system. After injection of Lipo@IR780/L012 nanoparticles, FUS was conducted with repetition frequency of 1 Hz (100 ms FUS on, 900 ms FUS off) and amplitude 60%. Animals were sacrificed 7 days after stimulation. All plots show mean ± SEM unless otherwise mentioned. *P <0.05, **P<0.01, ***P<0.001, ****P<0.0001; ns, not significant.

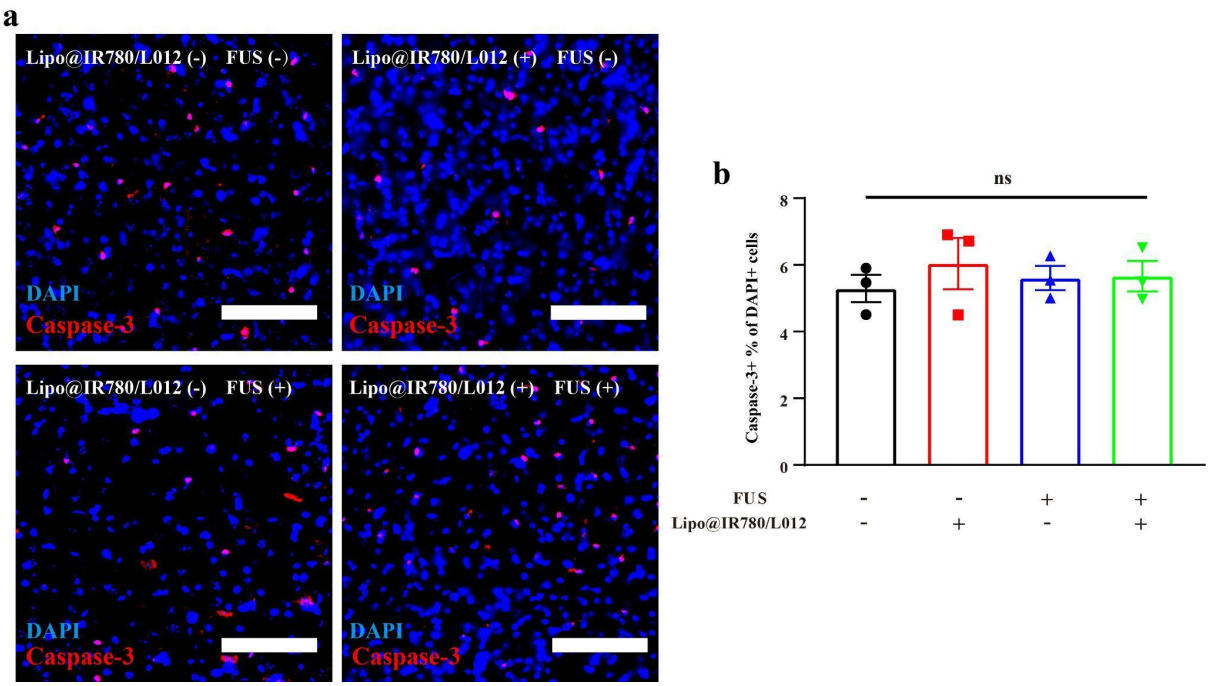

Figure S16. The biosafety assessment of our system in the motor cortex by immunostaining of Caspase-3 (marker of apoptosis in neuronal cells). (a) The immunostaining images in motor cortex area under the different stimulations; Scale bar: 100 μm. (b) Percentages of Caspase-3 positive cells within the cell population indicated by DAPI (n=3 per group, two-way ANOVA), indicating there was no obvious increase of apoptosis in neuronal cells under the treatment of this system. After injection of Lipo@IR780/L012 nanoparticles, FUS was conducted with repetition frequency of 1 Hz (100 ms FUS on, 900 ms FUS off) and amplitude 60%. Animals were sacrificed 7 days after stimulation. All plots show mean ± SEM unless otherwise mentioned. *P <0.05, **P<0.01, ***P<0.001, ****P<0.0001; ns, not significant.

Reference

(1) Li, S.; Xie, X.; Wang, W.; Jiang, S.; Mei, W.; Zhang, Y.; Liu, S.; Yu, X. Choline Phosphate Lipid as an Intra-Crosslinker in Liposomes for Drug and Antibody Delivery under Guard. *Nanoscale* **2022**, *14* (6), 2277–2286.

(2) Jiang, S.; Wang, W.; Dong, L.; Yan, X.; Li, S.; Mei, W.; Xie, X.; Zhang, Y.; Liu, S.; Yu, X. Infrared Responsive Choline Phosphate Lipids for Synergistic Cancer Therapy. *Chemistry* **2021**, *27* (49), 12589–12598.

(3) Lu, X.; Feng, X.; Werber, J. R.; Chu, C.; Zucker, I.; Kim, J.-H.; Osuji, C. O.; Elimelech, M.

Enhanced Antibacterial Activity through the Controlled Alignment of Graphene Oxide Nanosheets. *Proc. Natl. Acad. Sci. U. S. A.* **2017**, *114* (46), E9793–E9801.
(4) Zhang, F.; Wang, L.-P.; Brauner, M.; Liewald, J. F.; Kay, K.; Watzke, N.; Wood, P. G.; Bamberg, E.; Nagel, G.; Gottschalk, A.; Deisseroth, K. Multimodal Fast Optical Interrogation of Neural Circuitry. *Nature* **2007**, *446* (7136), 633–639.
(5) Hochbaum, D. R.; Zhao, Y.; Farhi, S. L.; Klapoetke, N.; Werley, C. A.; Kapoor, V.; Zou, P.; Kralj, J. M.; Maclaurin, D.; Smedemark-Margulies, N.; Saulnier, J. L.; Boulting, G. L.; Straub, C.; Cho, Y. K.; Melkonian, M.; Wong, G. K.-S.; Harrison, D. J.; Murthy, V. N.; Sabatini, B. L.; Boyden, E. S.; Campbell, R. E.; Cohen, A. E. All-Optical Electrophysiology in Mammalian Neurons Using Engineered Microbial Rhodopsins. *Nat. Methods* **2014**, *11* (8), 825–833.
(6) Wang, W.; Jiang, S.; Li, S.; Yan, X.; Liu, S.; Mao, X.; Yu, X. Functional Choline Phosphate Lipids for Enhanced Drug Delivery in Cancer Therapy. *Chem. Mater.* **2021**, *33* (2), 774–781.
(7) Wang, W.; Wang, B.; Ma, X.; Liu, S.; Shang, X.; Yu, X. Tailor-Made pH-Responsive Poly(choline Phosphate) Prodrug as a Drug Delivery System for Rapid Cellular Internalization. *Biomacromolecules* **2016**, *17* (6), 2223–2232.
(8) Wang, W.; Wang, B.; Liu, S.; Shang, X.; Yan, X.; Liu, Z.; Ma, X.; Yu, X. Bioreducible Polymer Nanocarrier Based on Multivalent Choline Phosphate for Enhanced Cellular Uptake and Intracellular Delivery of Doxorubicin. *ACS Appl. Mater. Interfaces* **2017**, *9* (19), 15986–15994.
(9) Wu, X.; Zhu, X.; Chong, P.; Liu, J.; Andre, L. N.; Ong, K. S.; Brinson, K., Jr; Mahdi, A. I.; Li, J.; Fenno, L. E.; Wang, H.; Hong, G. Sono-Optogenetics Facilitated by a Circulation-Delivered Rechargeable Light Source for Minimally Invasive Optogenetics. *Proc. Natl. Acad. Sci. U. S. A.* **2019**, *116* (52), 26332–26342.
(10) Nieuwenhuis, B.; Haenzi, B.; Hilton, S.; Carnicer-Lombarte, A.; Hobo, B.; Verhaagen, J.; Fawcett, J. W. Optimization of Adeno-Associated Viral Vector-Mediated Transduction of the Corticospinal Tract: Comparison of Four Promoters. *Gene Ther.* **2021**, *28* (1-2), 56–74.
(11) Nagase, A.; Takahashi, M.; Nakano, M. Automatic Calculation and Visualization of Nuclear Density in Whole Slide Images of Hepatic Histological Sections. *Biomed. Mater. Eng.* **2015**, *26 Suppl 1*, S1335–S1344.
(12) Nagato, Y.; Kondo, F.; Kondo, Y.; Ebara, M.; Ohto, M. Histological and Morphometrical Indicators for a Biopsy Diagnosis of Well-Differentiated Hepatocellular Carcinoma. *Hepatology* **1991**, *14* (3), 473–478.
(13) Nath, T.; Mathis, A.; Chen, A. C.; Patel, A.; Bethge, M.; Mathis, M. W. Using DeepLabCut for 3D Markerless Pose Estimation across Species and Behaviors. *Nat. Protoc.* **2019**, *14* (7), 2152–2176.